Experimental and Numerical Studies in a Vortex Tube

Chang-Hyun Sohn*, Chang-Soo Kim
School of Mechanical Engineering,
Kyungpook National University Daegu 702-701, Korea
Ui-Hyun Jung
SL Co., 1208-6, Sinsanri, Jinyang-up, Kyungsan, Kyungpouk 712-837, Korea
B. H. L Lakshmana Gowda
School of Mechanical Engineering,
Kyungpook National University, Daegu 702-701, Korea

The present investigation deals with the study of the internal flow phenomena of the counter-flow type vortex tube using experimental testing and numerical simulation. Visualization was carried out using the surface tracing method, injecting dye on the vortex tube wall using a needle. Vortex tube is made of acrylic to visualize the surface particle tracing and the input air pressure was varied from 0.1 MPa to 0.3 MPa. The experimentally visualized results on the tube show that there is an apparent sudden changing of the trajectory on the vortex tube wall which was observed in every experimental test case. This may indicate the stagnation position of the vortex flow. The visualized stagnation position moves towards the vortex generator with increase in cold flow ratio and input pressure. Three-dimensional computational study is also conducted to obtain more detailed flow information in the vortex tube. Calculated total pressure, static pressure and total temperature distributions in the vortex tube were in good agreement with the experimental data. The computational particle trace on the vortex tube wall is very similar to that observed in experiments.

Key Words : Vortex tube, Energy Separation, Visualization, Stagnation Point

1. Introduction

The vortex tube is a structurally simple energy separation device for compressed gas stream to separate the flow into cold and hot gas streams, without moving parts or any chemical reactions. This device consists of a simple circular tube, nozzle and throttle valve. Compressed air enters the vortex tube tangentially through the vortex generator and develops vortex flow. The injected air is forced towards the tube wall by the

influence of the centrifugal forces and the air is heated by dissipation and heat transfer, mainly near the wall. This energy separation phenomenon by vortex tube has attracted interest from various points of view such as, simple structure, non-moving parts and no chemical reactions. Additionally, the vortex tube can be used as a cooling device without creating any environmental problems. Taking advantage of this simple structure and operation, vortex tube has been applied to air-cooled suits in the high temperature work environments as well as being used as a cooling device for cutting tools and electronic equipment. Successful use of the vortex tube in these fields has been limited by a poor understanding of the fundamental thermo-fluid mechanism that governs the energy separation phenomena, due to the complexity of the problem and the difficulty of

---
* Corresponding Author,
  E-mail : chsohn@knu.ac.kr
  TEL : +82-53-950-5570; **FAX** : +82-53-950-6550
  School of Mechanical Engineering, Kyungpook National University, 1370 Sangyeok-dong, Buk-gu, Daegu 702-701, Korea. (Manuscript **Received** May 26, 2005; **Revised** January 18, 2006)

obtaing reliable experimental results.

Many studies on the vortex tube have been conducted since the Ranque's patent(1932). Hilsh (1947) investigated the influence of geometrical configuration of the vortex tube with regard to energy separation. Kassner and Knoernschild (1948) proposed a flow pattern in the vortex tube. Hartnett and Eckert (1957) measured the flow pattern and total temperature in the vortex tube and proposed a theory of energy separation in the vortex tube. Ogawa (1993) assumed that a lump of fluid moves to another radial position because of the development of fluid instability which induces isentropic compression and expansion in the vortex tube. Choi and Riu (1996) measured the maximum wall temperature along the vortex tube surface providing useful information about the location of the stagnation point of the flow field at the axis of the vortex tube. Ahlborn and Groves (1997) measured the axial and azimuthal velocities by pitot probe and proposed the existence of secondary circulation flow in the vortex tube. They reported the difficulty of using a non-invasive measurement method, LDV, due to high centrifugal acceleration. Frohlingsdorf and Unger (1999) numerically simulated the compressible flow and energy separation phenomena using the commercial code CFX. They calculated the flow phenomena as an axisymmetric flow.

Despite the various investigations performed on the vortex tube, the fundamental mechanism of the phenomenon involved is still not clear. The purpose of this study is to investigate the phenomena of the vortex tube using flow visualization and three-dimensional computational method.

2. Experimental Apparatus and Results

Figure 1 shows a schematic diagram of the experimental apparatus for the vortex tube experiments. It consists of the three components viz, input air supply parts, test section and data processing unit. Air supply parts consist of air-compressor ①, 40 μm mesh sized pre-filter ②, after-cooler ③, main-filter ④ and the air-dryer ⑤. Pressure-regulator ⑥ is provided at the front

of vortex tube generator to supply constant pressured air. Input air pressure is measured by a pressure module ⑦.

More details of the test section ⑧ are shown in Fig. 2. Vortex tubes are made of pyrex to visualize the flow trajectory on the wall. The tested vortex tube is counter flow type and a simple type of vortex generator is adopted. Table 1 shows the detailed dimensions of the vortex tube. Visualization was carried out by the surface tracing method, injecting dye on the vortex tube wall through a needle (27G). The needle was installed between two acrylic-plates which are bolted with o-ring to prevent leakage of air. The
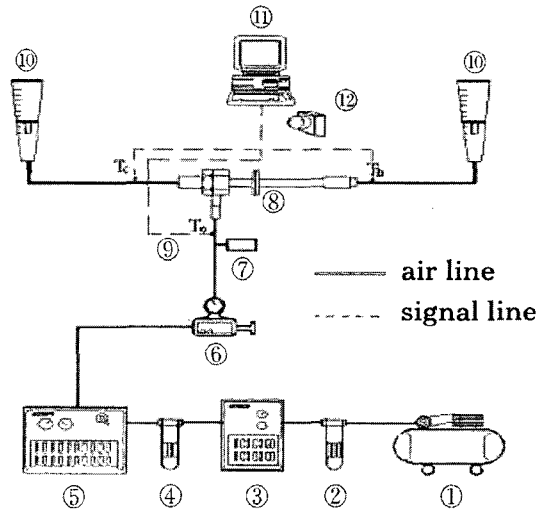
① Compressor ② Pre filter ③ After cooler ④ Main filter ⑤ Air dryer ⑥ Regulator ⑦ Pressure gauge ⑧ Vortex tube ⑨ Thermocouple ⑩ Flow meter ⑪ P.C. ⑫ Camera

Fig. 1 The schematic diagram of experimental apparatus
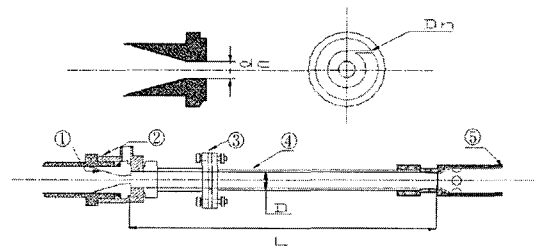
① Vortex generator ② Housing ③ Dye injector ④ Tube ⑤ Throttle valve

Fig. 2 The schematic diagram of vortex tube

Table 1 Dimensions of vortex tube

Tube diameter (D)	20 mm
Tube length (L)	600 mm
Hydraulic diameter of vortex generator (Dn)	5.7 mm
Cold air output orifice diameter (D_c)	8.9 mm
Nozzle area ratio (Sn)	0.155
Vortex chamber diameter ratio	1
Cold air orifice diameter ratio (ζ)	0.446
Dimensionless length	30

position of dye-injection is located at a distance of 5D from the vortex generator based on the experimental results of Takahama (1966). He noted that the axially symmetric flow was fully developed after a length of 3D from the vortex generator.

K-type thermocouples ⑨ are positioned at air inlet, hot and cold outlet of vortex tube. Before the test, thermocouple was calibrated within 0.1℃ by temperature calibrator (Calibrator-741B). Data processing unit was composed of data-acquisition board (AXIOM5412) and personal computer ⑪. The dye trajectories on the vortex tube have been photographed by camera ⑫ with 1/250 sec shot speed.

Experimental tests were conducted with a range of input pressure from 0.1 MPa to 0.3 MPa. The cold air flow ratio (y=cold flow rate/input flow rate) was varied from 0.3 to 0.9 for each input pressure case by adjusting the throttle valve. The
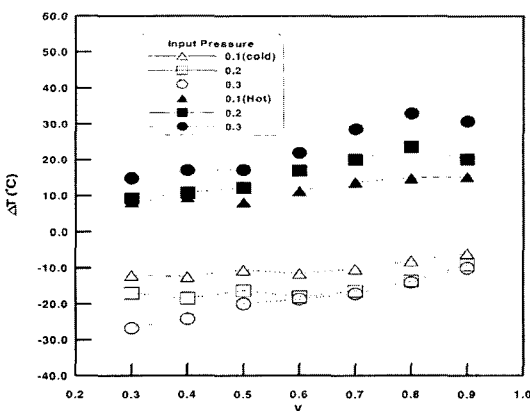
inlet air temperature was set to 27℃. The dye was injected after the cold and hot air temperatures attained a steady state. The steady state was determined to be when the change of temperatures was within ±0.2℃.

Figure 3 shows the cold ($\triangle T_c = T_{atm} - T_{cold}$) and hot temperature difference ($\triangle T_h = T_{atm} - T_{hot}$) with different inlet air pressure and cold flow ratio (y=cold flow rate/input flow rate). With an increase in the input pressure, the difference ($\triangle T_h - \triangle T_c$) increases which also indicates the performance of the vortex tube in energy separation.

Figure 4 shows the flow trajectory of dye on the vortex tube wall with inlet air pressure of p=0.1 MPa for y=0.3 to 0.7. Figure 5 shows the flow trajectory lines on the vortex tube for a fixed cold flow ratio (y=0.5) with different inlet air pressure. It is observed that there is a sudden change of trajectory on the vortex tube wall in every experimental test case. The sudden change position of the trajectory moved towards the vortex generator as the cold flow ratio increased (Fig. 4) and inlet air pressure increased (Fig. 5). However it is observed that the change in Ls (Fig. 5) is smaller between p=0.2 to 0.3 Mpa compared to that between p=0.1 to 0.2 Mpa.

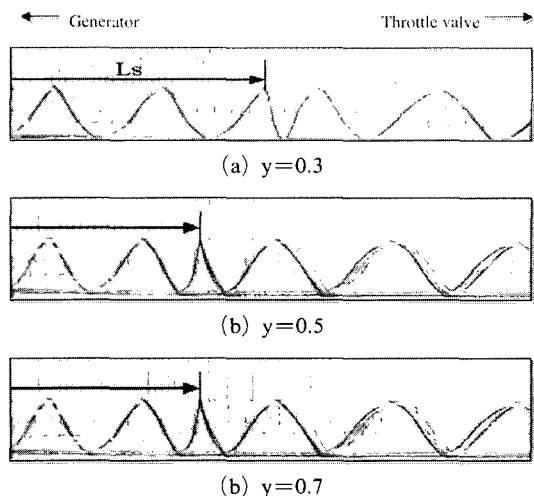Fulton (1950) proposed a 2-D flow pattern in the vortex tube with a stagnation point in the cen-

Fig. 3 Cold and hot temperature difference with cold air flow ratio (y)

(a) y=0.3

(b) y=0.5

(b) y=0.7

Fig. 4 Photographs of dye trajectory on the vortex tube wall (p=0.1 MPa)
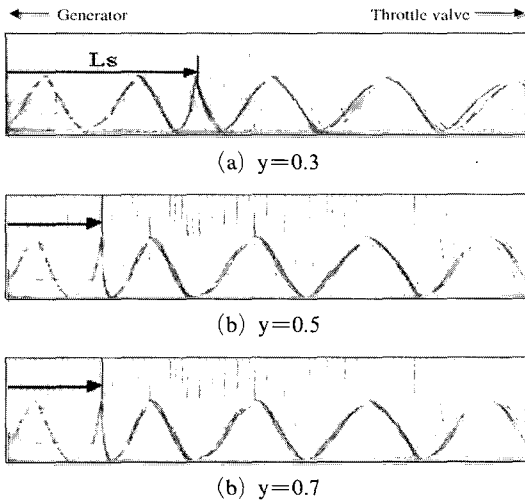
Fig. 5 Photographs of dye trajectory on the vortex tube wall (y=0.5)

(a) y=0.3

(b) y=0.5

(b) y=0.7

Fig. 6 Distributions of wall temperature profile with various cold flow ratio at 0.1 MPa

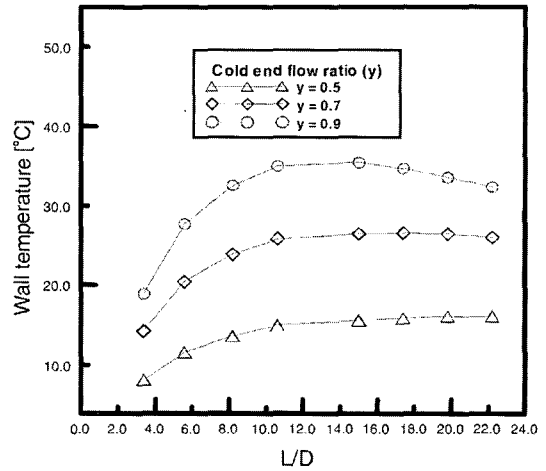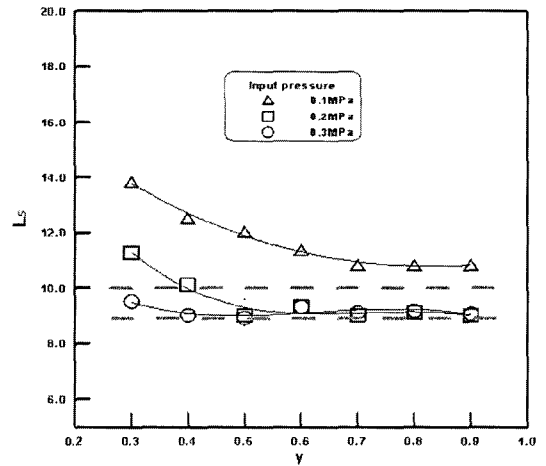Fig. 7 The dimensionless length of stagnation point as a function of the flow rate ratio

tral region of the vortex tube. The sudden change in position of the trajectory on the tube wall may be strongly related to the stagnation point on the central region of the vortex tube. Since the stagnation point is a position of maximum static pressure and the flow towards the throttle valve is retarded, i.e., the axial velocity decreases near the stagnation position.

Choi and Riu (1996) measured the wall temperature along the vortex tube surface and reported that the maximum wall temperature position is related to the location of the stagnation point of the flow field at the axis of the vortex tube. Figure 6 shows the measured wall temperature distribution with various cold flow ratios at 0.1 Mpa condition. There may be a strong correlation between the temperature increase and the stagnation position but it is difficult to indicate the location of the stagnation position from the wall temperature distribution since the profile of wall temperature near the stagnation position is very flat.

In Figs. 4 and 5, Ls is assigned to indicate the stagnation length from the vortex generator to stagnation point. Figure 4(c) shows additional sudden compression. It may be strongly related with periodic compression and expansion near hot end since there exists strong adverse pressure gradient. Figure 7 shows that the dimensionless

length of stagnation position moves towards the vortex generator as the cold flow ratio increases and the inlet air pressure increases. However at inlet air pressures higher than 0.2 MPa, the stagnation position is nearly constant at 9D from the inlet in the present investigation.

3. Numerical Analysis

The three-dimensional flow field in a vortex tube was numerically studied using a commercial code, CFD-ACE, which utilizes a finite volume method to handle compressible flows. To verify

the above computational method, the vortex tube problem was solved using steady three-dimensional Navier–Stokes equations with the standard k–ε turbulence model and a third order upwind scheme.

Figure 8 along with Table 2 shows the Hartnett's experimental vortex tube geometry and dimensions. This was used as the basic geometry for the simulations. Figure 9 indicates the grid system used in this study near the vortex generator. Hartnett's experiment was performed with zero cold flow rate $(y=0)$; accordingly the computational boundary condition at the cold outlet boundary was taken as a wall condition and the

inlet boundary condition was the same as that in Hartnett's experiments. The hot outlet boundary condition was given as the atmospheric pressure condition as indicated in Table 3.

Table 3 Boundary conditions for Hartnett's experiment

Inlet condition	Cold outlet	Hot outlet
Fixed total pressure & total temperature P=20psig T=300K	Wall condition	Fixed atmospheric pressure

Table 2 Hartnett's experimental dimensions of a vortex tube

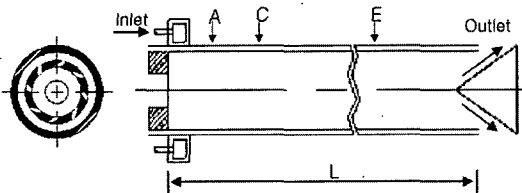|	
Tube diameter (D)	3 inch
Tube length (L)	30 inch
Nozzle diameter (Dn)	0.375 inch
Angle of cone–shaped valve	60 degree
Number of nozzle	8
Dimensionless length (L/D)	10

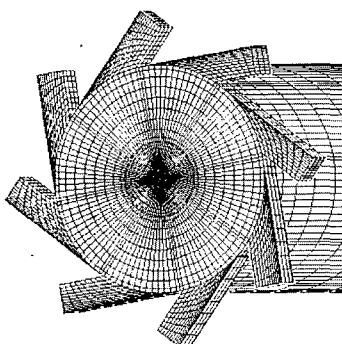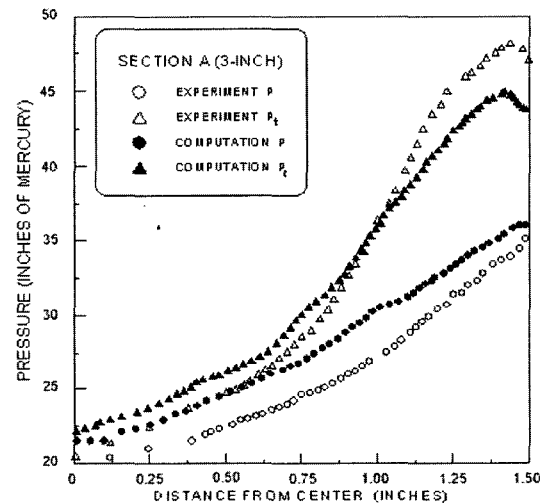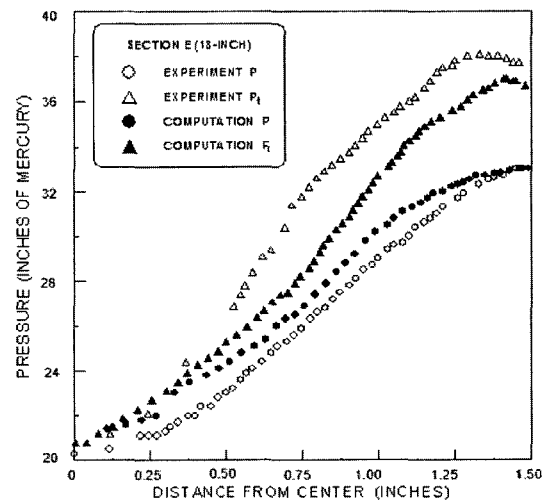**Fig. 8** Hartnett's experimental geometry of a vortex tube

Fig. 9 Grid near vortex generator of Hartnett's test vortex tube

(a) Section A

(b) Section E

Fig. 10 Comparison of calculated pressure with Hartnett's experimental data

Figures 10 and 11 show the comparison of calculated results with Hartnett's experimental total pressure and static pressure distributions at various sections as indicated in Fig. 8. The computed results are in good agreement with the experimental ones.

Since Hartnett's experiments were performed with zero cold flow rates, computational analysis was conducted with the identical conditions for the present experimental case. Figure 12 shows a detail grid system near the vortex generator and at the hot outlet. Grid independency was checked

with different number of grids and finally about 120,000 grid points were made use of. The inlet total pressure is fixed as 0.3 MPa and the hot outlet area was adjusted to match the cold flow ratio (y). Table 4 shows that the calculated cold ($\triangle T_c$) and hot temperature difference ($\triangle T_h$), are in good agreement with the experimental results.

Table 4 Comparison of computed temperature difference with experimental results

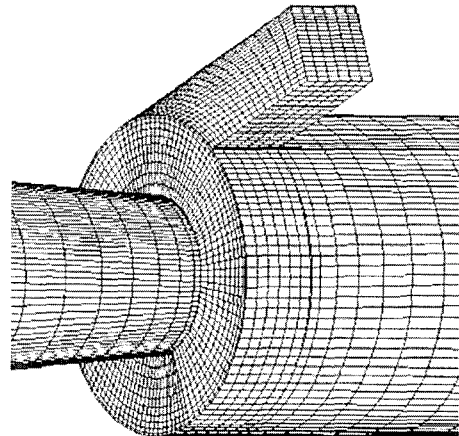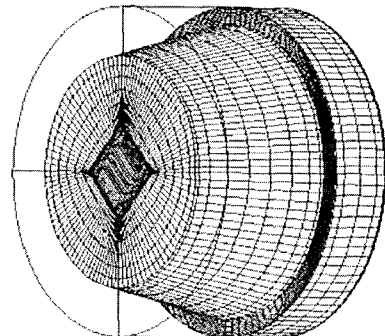| Cold flow ratio	$\triangle T_C(^\circ C)$		$\triangle T_H(^\circ C)$	
	Exp.	Cal.	Exp.	Cal.
0.55	−19.5	−19.8	20.0	20.1
0.6	−17.2	−19.1	25.0	23.4
0.7	−16.5	−17.2	27.0	27.3
0.8	−15.1	−15.7	32.0	29.1
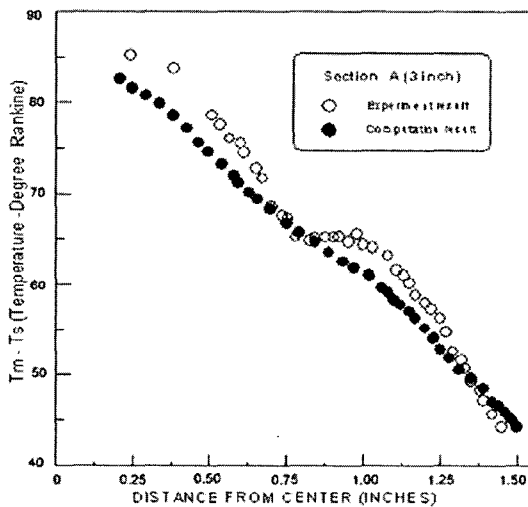
(a) Section A
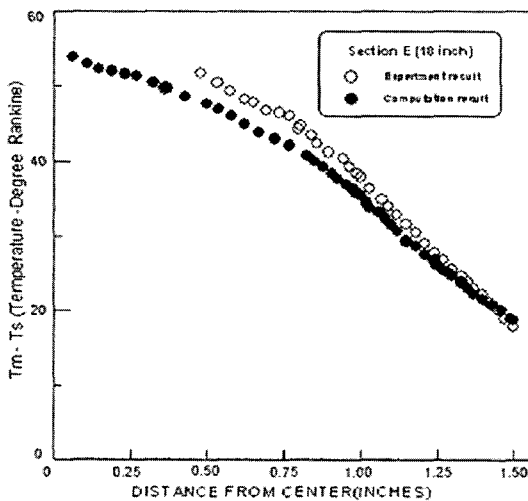
(b) Section E

Fig. 11 Comparison of calculated temperature with Hartnett's experimental data

(a) Grid near the vortex generator

(b) Grid near hot outlet

Fig. 12 Grid near vortex generator and hot outlet

Figure 13(a) shows the particle traces of cold and hot flow near vortex generator. The computational velocities show that the rotating direction of cold flow in central position of vortex tube is same direction of the outer hot flow but the axial velocity of cold and hot flow are counter to the direction of each other. Figure 13(b) shows the computed velocities near stagnation position and particle trajectory line on the tube wall. The computed central axial velocities change from negative direction to positive direction and the stagnation position is coincided with the computed sudden change position of particle trajectory line on the vortex tube wall.

Figure 14 shows the cross sectional velocity vectors at the vortex generator, L/D=4 and L/D=8. The rotating flow center is not matching with the geometric center and the offset is reducing towards the throttle exit.

Figure 15(a) shows the computational particle trace on the vortex tube wall and velocity vector with different cold flow ratio (y). It is observed that there is a sudden change in the position of particle trace on the vortex tube wall. This position coincides with the stagnation point in the central region of the vortex tube and it moves towards the cold flow exit with increase of y value. The calculated results are very similar to the experimental results shown in Fig. 15(b).
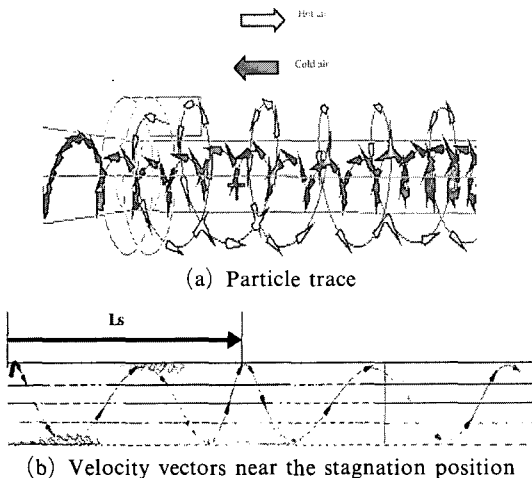
Strong circulation is generated by vortex generator at positions near the cold end, and the primary vortex stream flows towards the hot end like the
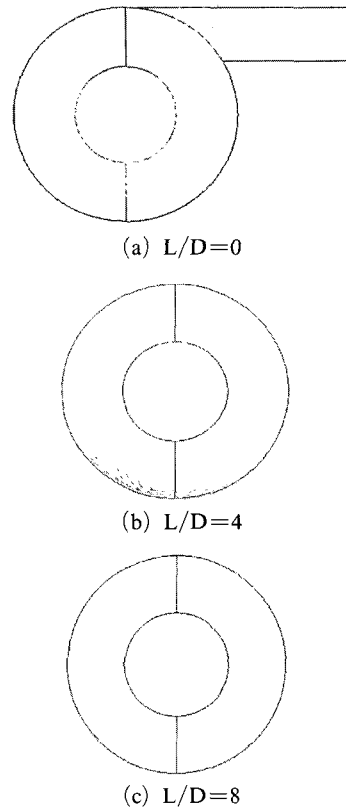

(a) L/D=0

(b) L/D=4

(c) L/D=8

Fig. 14 Computational velocity vectors at cross section

(a) Particle trace

(b) Velocity vectors near the stagnation position

Fig. 13 Computational particle trace and velocity vectors near the stagnation position

(a) Computational particle trace on the wall and velocity vector

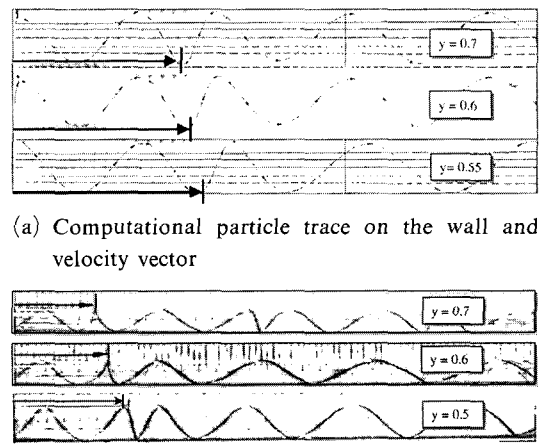(b) Experimental particle trace on the wall

Fig. 15 Comparisons of particle trace on the wall

spiral lines on a corkscrew as shown in Fig. 13 (a). As the throttle valve allows only the flow in the outer region, the gas speed of inner region decreases and generate the stagnation region. If the inlet pressure increases, the pressure drop between inner vortex tube and outer atmosphere also increases and it generates greater adverse pressure gradient towards the hot end and higher favorable pressure gradient towards the cold end for the inner region gas. Because of these pressure gradients, the stagnation position moves towards the vortex generator.

4. Conclusions

In this study the flow phenomena in the counter-flow type vortex tube is investigated by experiments and numerical simulation. The experiments were conducted over a range of input pressure, from 0.1 MPa to 0.3 MPa, and the cold flow ratio is changed from 0.3 to 0.9 for each input pressure case. Visualization was carried out by the surface tracing method, injecting dye on the vortex tube wall through a needle.

It was found that there is a sudden change in the position of the trajectory on the vortex tube wall in every experimental test case. The sudden changing position of trajectory on the wall is due to the stagnation position of cold flow in the central region of vortex tube. However, it is difficult to indicate the location of stagnation position. The stagnation position moves towards the vortex generator as the cold flow ratio increases at inlet air pressure of 0.1 MPa. Also the stagnation position moves towards the vortex generator as the inlet air pressure increases from 0.1 MPa to 0.3 MPa. However, at inlet air pressures higher than 0.2 MPa, in this experimental study, the stagnation position is nearly fixed at 9D length.

Three-dimensional computational study is also conducted to obtain more detailed flow information in the vortex tube. Computed total pressure, static pressure and total temperature distributions in the vortex tube are in good agreement with the experimental data. The computational particle trace on the vortex tube wall is very similar to that observed in experiments.

Acknowledgments

References

Ahlborn, B. and Groves, S., 1997, "Secondary Flow in a Vortex Tube," *Fluid Dynamics Research*, Vol. 21, pp. 73~86.

Choi, B. C. and Riu, K. J., 1996, "An Experimental Study for Cold End Orifice of Vortex Tube," *Transaction of the KSME B in Korea*, Vol. 20, No. 3, pp. 1061~1073.

Frohlingsdorf, W. and Unger, H., 1999, "Numerical Investigations of the Compressible Flow and the Energy Separation in the Ranque-Hilsch Vortex Tube," *International Journal of Heat and Mass Transfer*, Vol. 42, pp. 415~422.

Fulton, C. D., 1950, "Ranque's Tube," *Refriug. Eng.*, Vol. 5, pp. 473~479.

Hartnett, J. P. and Eckert, E. R. G., 1957, "Experimental Study of the Velocity and Temperature Distribution in a High-Velocity Vortex-Type Flow," *Trans. ASME*, Vol. 79, No.4, pp. 751~758.

Hilsh, R., 1947, "The Use of Expansion of Gases in a Centrifugal Field as a Cooling Process," *Review of Scientific instruments*, Vol. 8, No. 2 pp. 108~113.

Kassner, R. and Knoernschild, E., 1948, "Friction Laws and Energy Transfer in Circular Flow," *U.S.A.F. Air Material Command Wright-Patterson* AFB, Proj. March, NO. LP-259, Tech. Rept. NO. FCR-2198-ND, GS-US-AF,AF Base NO. 78.

Ogawa, A., 1993, *Vortex Flow*, CRC Press, pp. 272~277.

Ranque, G. J., 1932, *United State Patent*, Applied December 6. Serial No. 646.020.

Takahama, H., 1966, "Experimental Study of Vortex Tube," *Bulletin of JSME*, Vol. 9, No. 33, pp. 227~245.